Prediction of Broadband Noise from Symmetric and Cambered Airfoils

Vasishta BHARGAVA*,[1], Rahul SAMALA[2], Chandramouli ANUMULA[3]

*Corresponding author
*,[1]Sreyas Institute of Engineering and Technology, India,
Besides Indu Aranya, GSI, Bandlaguda, Nagole, Hyderabad – 500068
vasishtab@gmail.com
[2]Indian Institute of Technology,
Chennai, Tamil Nadu, 600036, India
[3]KL University, India,
Green Fields, Guntur District, Vaddeswaram, Andhra Pradesh 522502, India

DOI: 10.13111/2066-8201.2019.11.1.3

Received: 20 December 2018/ Accepted: 03 February 2019/ Published: March 2019

Abstract: *Aerodynamic sound generation and self-noise mechanisms from lifting surfaces such as airfoil involve the fields of classical acoustics and fluid mechanics. In this paper, trailing edge noise production is evaluated using empirical model for NACA 0012 and NACA 6320 airfoils. The sound pressure levels from trailing edge surface are calculated for different flow configurations. The growth of boundary layer thickness and displacement thickness, for different chord lengths and Mach numbers with varying angles of attack, is illustrated for NACA 0012. The sound pressure levels were computed numerically between 0^0 to 6^0 angles of attack and at constant chord length of 1.2m using Brookes Pope Marcolini method. The results showed a change of ~2-5dB in peak amplitude for mid frequencies region of spectrum. The effects of varying chord length and Mach number on sound pressure levels are illustrated for both airfoils. The relative velocity field for airfoils was computed using the boundary element method. The combined effect of thickness and camber on sound power level is demonstrated at a 4^0 angle of attack and for a Mach number of 0.191. Validation of sound pressure levels is done based on the results obtained for NACA0012 for similar flow conditions.*

***Key Words*:** *Airfoil, Noise, Sound Pressure Level, Trailing edge, Boundary layer thickness*

1. INTRODUCTION

Noise is unwanted sound that is produced due to pressure disturbances in atmosphere relative to standard atmospheric pressure. The thresholds of hearing and pain for a human are 0dB and 140dB in audible frequency spectra. Many engineering structures produce noise when they interact with atmospheric air during operation and cause annoyance to inhabitants in environment. Broadband aerodynamic noise contributes significantly to the overall sound pressure levels as a result of rotating components such as blades of the wind turbine, fan, compressor etc. Airborne and structural borne noise are two different noise sources that depend upon the aerodynamic and structural properties of material. One of the contributors to sound radiation is the unsteady fluid motion and shear stress within the flow that act as weak source of sound [9]. Velocity fluctuations within turbulent boundary layer flow are

responsible for wall pressure changes as a result of interaction with the rigid and flat surfaces. The wall pressure fluctuations also contribute to noise in applications such as aircraft cabin noise, during transportation [7], [8] The wall pressure spectrum has been studied by several researchers [7 - 13]. They have shown that the boundary layer turbulence along the walls depends on fluctuating velocity component as well as on the mean flow values. The main factors involved in the flow induced noise radiation from the aircraft cabins are due to the inflow turbulence impinged on the fuselage, relative to the free stream velocity. Hence important broadband noise sources coming from the aircraft components like landing gear, wing span sections such as slat, flaps and engine casing or even jet noise, blades of wind turbine depend to a large extent on the geometric variables, boundary layer properties as well as on the free stream velocity. The source characterization can be attributed to the characteristic dimension of the source such as chord length, trailing edge thickness, and boundary layer thickness compared with wavelength of acoustic waves. Therefore, sources are treated as either non compact or compact forms when the acoustic wavelength exceeds the characteristic dimension. So, the characteristic wall pressure fluctuations determine to a large extent the nature of the noise source and acoustic pressure levels which affect the ergonomics of flight. The earliest empirical models for predicting sound spectrum were based upon the wind tunnel experimentation conducted by [2], [3] who used NACA 0012 and NACA 0018 airfoils with chord lengths up to 0.5m, for measuring the surface pressure fluctuations, boundary layer properties and far field noise spectra. The measured data enabled to understand the mechanism responsible for broadband noise caused by the interaction of the turbulent boundary layer and the external pressure gradients over the trailing edge airfoil surface [2], [3], [16]. Inferences were drawn that flow separation on airfoil trailing edge due to adverse pressure gradient contributes to the acoustic pressure and it was found varying with angles of attack. Experiment studies of [2], [3] also provided necessary background for deriving the curve fitting equations for boundary layer thickness, displacement thickness and momentum thickness expressed as function of angle of attack and chord Reynolds number [3]. In this paper, the effect of chord length and Mach number, on trailing edge noise from NACA 0012 and NACA 6320 airfoils with thickness to chord ratio of 12 % and 20 % is evaluated through computer simulation using BPM model. The objective of the study was to illustrate the sound pressure level patterns by varying the airfoil chord length and the free stream Mach numbers. The effect of the airfoil thickness and camber on trailing edge noise caused by edge scattering of turbulent boundary layer is demonstrated. The development of the boundary layer thickness and the displacement thickness for NACA 0012 and NACA 6320 airfoils are also shown for suction and pressure sides from 0^0 to 25^0angle of attack for varying chord lengths and Mach numbers flow conditions.

2. COMPUTATIONAL FRAMEWORK

The simulation is based on the 2D incompressible flow over the airfoils NACA 0012 and NACA 6320, respectively. The assumptions document is based on prediction model (BPM) and the program script for simulation was developed in MATLAB 2017b software.

The important parameters are the chord length, the angle of attack, the receiver location, and the free stream velocities of 65m/s and 40m/s. corresponding to the chord Reynolds number (Re), of 3.134×10^6, 4.612×10^6.

For the present analysis, a moderate range of angle of attack was chosen up to 6^0 and chord lengths for 1.2m, 0.5m and 0.8m for constant span of 2m. The program utilizes the

aerodynamic and geometric data of airfoils to compute the relative velocity on the surface of airfoils. Pilot simulation runs were conducted at each angle of attack and for varying chord lengths to verify the accuracy of the output data *(numeric MAT files)* with existing analytical data available from reference [2], [3]. From past studies, the sound pressure levels have been found maximum for the downwind receiver location and hence for all computations it is taken as worst case scenario [1], [3], [4].

The primary reason attributed to downwind position was related to the refraction of sound waves in downward direction with respect to free stream velocity direction. This phenomenon is referred to as amplitude modulation or amplification of sound waves which results in broadband noise from airfoils or airfoils integrated to a blade as found in wind turbines [4]. Fig. 1 shows the overall scheme of implementation for the simulation work of assessing the trailing edge noise from airfoils.

For pilot runs, a set of simulation runs with varying span and chord lengths were performed and output data were verified for accuracy with model assumptions document. The required changes to the geometry and flow parameters were done in order to ensure accuracy within +/- 5% of existing empirical data. Finally, the configuration for both airfoils was done and output data logged in form of MAT files.

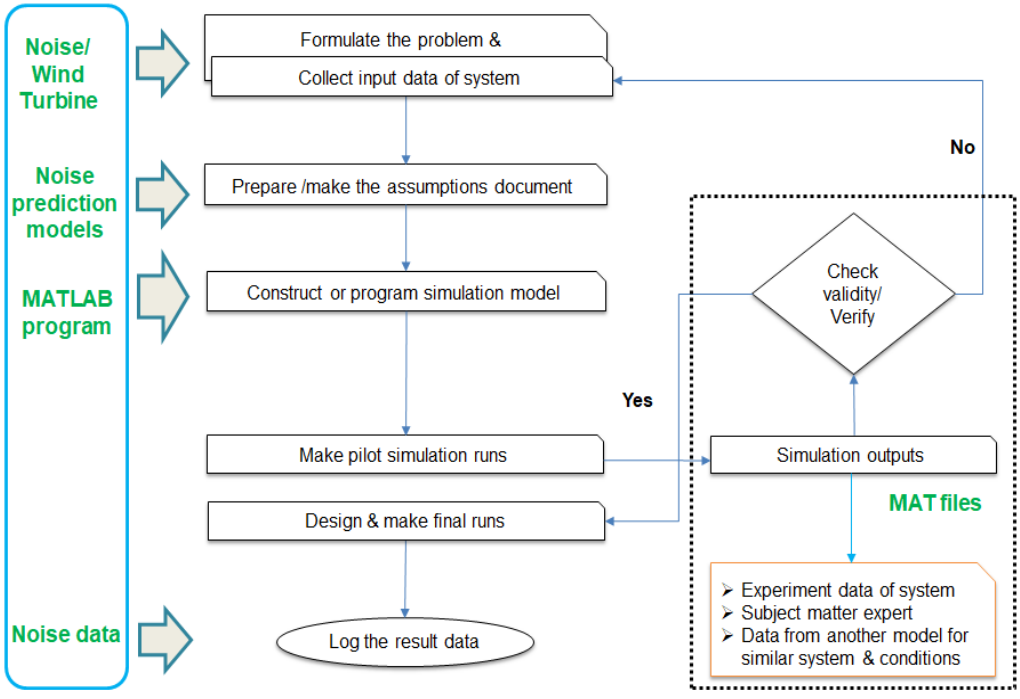

Figure 1. Illustration of computational framework implemented for noise prediction method

3. MODEL DESCRIPTION

The empirical method is based on the curve fitting expressions for boundary layer parameters viz. thickness and displacement thickness which are derived from the wind tunnel experiment data and given by Eq. (2) - Eq. (16) in ref [2], [3].

The equations of the empirical model for evaluating the sound pressure level from the contributing pressure, suction, separation noise sources and the total turbulent boundary layer trailing edge noise source are shown in Eq. (1) to Eq. (4):

$$\mathrm{SPL_p} = 10.\log 10\left[\frac{\delta_{\mathrm{p}}^{*}\mathrm{M}^{5}\mathrm{L}\overline{\mathrm{D_h}}}{\mathrm{r_e^2}}\right] + \mathrm{A}\left[\frac{\mathrm{St_p}}{\mathrm{St_1}}\right] + [\mathrm{K1} - 3] + \Delta\mathrm{K1} \tag{1}$$

$$\mathrm{SPL}_s = 10.\log 10\left[\frac{\delta_{s}^{*}\mathrm{M}^{5}\mathrm{L}\overline{\mathrm{D_h}}}{\mathrm{r_e^2}}\right] + \mathrm{A}\left[\frac{\mathrm{St_s}}{\mathrm{St_1}}\right] + [\mathrm{K1} - 3] \tag{2}$$

$$\mathrm{SPL}_{\alpha} = 10.\log 10\left[\frac{\delta_{\mathrm{s}}^{*}\mathrm{M}^{5}\mathrm{L}\overline{\mathrm{D_h}}}{\mathrm{r_e^2}}\right] + \mathrm{B}\left[\frac{\mathrm{St_s}}{\mathrm{St_2}}\right] + \mathrm{K2} \tag{3}$$

$$\mathrm{SPL_{Total}} = 10.\log 10\left[10^{\frac{\mathrm{SPL}_{\alpha}}{10}} + 10^{\frac{\mathrm{SPL_p}}{10}} + 10^{\frac{\mathrm{SPL_s}}{10}}\right] \tag{4}$$

The Strouhal number and Reynolds number definitions are given by Eq. (5) to Eq. (8) and Eq. (9) and Eq. (10):

$$\mathrm{St}_p = \left[\frac{\mathrm{f}\delta_{p}^{*}}{\mathrm{U}}\right] \tag{5}$$

$$\mathrm{St}_s = \left[\frac{\mathrm{f}\delta_{s}^{*}}{\mathrm{U}}\right] \tag{6}$$

$$\mathrm{St_1} = \mathrm{St_2} = [0.02M^{-0.6}] \tag{7}$$

$$\mathrm{St_{avg}} = \left[\frac{\mathrm{St_1} + \mathrm{St_2}}{2}\right] \tag{8}$$

$$\mathrm{Re}_p = \left[\frac{\delta_{p}^{*}U}{\vartheta}\right] \tag{9}$$

$$\mathrm{Re_c} = \left[\frac{\mathrm{Uc}}{\vartheta}\right] \tag{10}$$

The logarithmic scaling laws for determining the sound pressure use the Strouhal numbers, chord Reynolds number, Reynolds number and dependent upon frequency, *f*, displacement thickness, δ^*, L- span length of airfoil, M – Mach number.

It is clear that prediction for sound pressure varies as inverse square relation between the receiver and source distance, r_e.

The interpolating shape functions for sound spectrum are denoted by A and B. The function A represents the suction and pressure sides from airfoil for trailing edge source and B for angle dependent source and evaluated using the equations.

The amplitude functions are given by K1, K2 and ΔK1 [2], [3]; ΔK1 is the amplitude modulating factor.

$\overline{\mathrm{D_h}}$ is the high frequency directivity function expressed in terms of directivity angles and convective Mach number given by Eq (B1) and Eq. (B2) in appendix of the references [2], [3].

Detailed equations for implementing boundary conditions necessary for model airfoil and interpolation factors required to analyze sound pressure levels are available in ref [1], [2], [3] [16].

The boundary layer equations are expressed in terms of chord length, c, angle of attack as well as chord Reynolds number $\mathrm{Re_c}$.

4. RESULTS & DISCUSSIONS

4.1 Geometry of Airfoil profiles and Pressure distribution

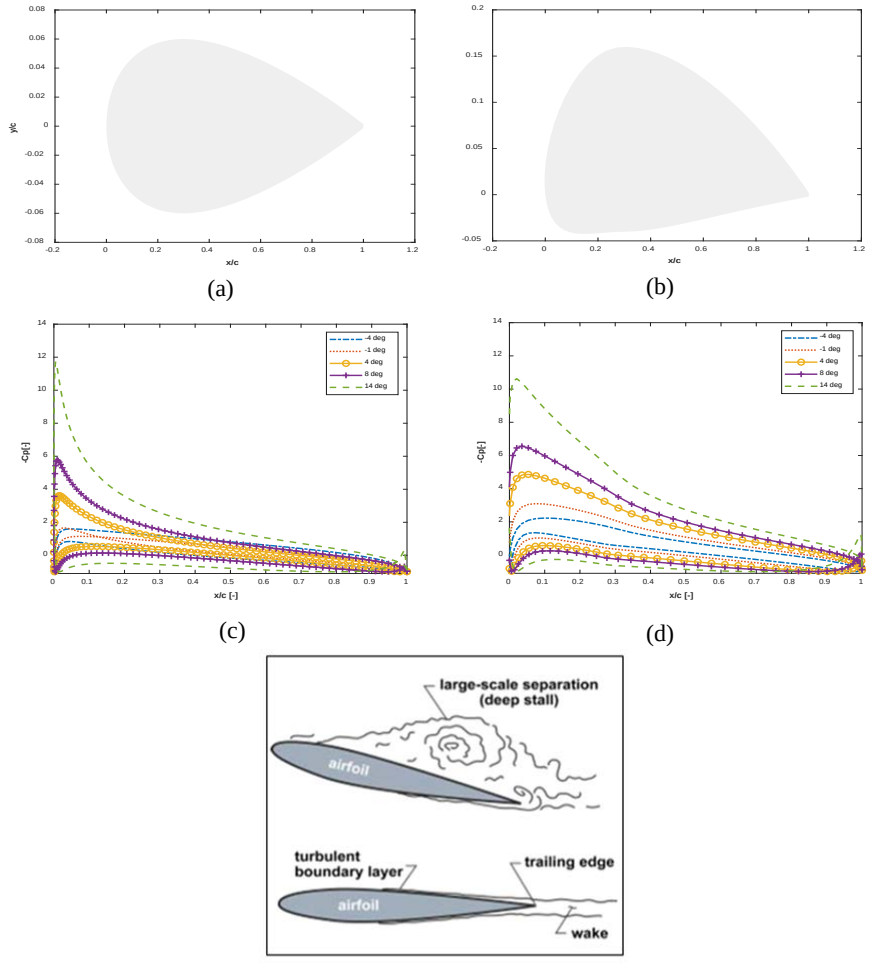

Figure 2. Geometry of (a) NACA 0012 (c) NACA 6320 (c) Cp for NACA 0012 (d) Cp for NACA 6320 (e) Illustration of turbulent boundary layer over the trailing edge of an airfoil [3]

Fig. 2(a) and Fig. 2(b) show the geometry of NACA 0012 and NACA 6320 airfoils. The surface pressure coefficient, C_p distribution for the profiles is shown in Fig. 2(c) and Fig. 2(d) for Reynolds number of 6.2 x 10^5.

The Cp values at angles of attack between -4^0 and 14^0 are evaluated using the viscous panel method as described in ref. [14] Fig. 2(e) illustrates the mechanism of TBL-TE on airfoil responsible for the sound radiation in the source region or far field.

Table 1. Geometric data of airfoils used for computational study

Parameter	NACA 0012	NACA 6320
Max. thickness	12 %	20%
Max. camber	-	6% of chord
Position of camber	-	3/10th of chord from LE
Type of airfoil	Symmetric	Cambered

4.2 Effect of chord length

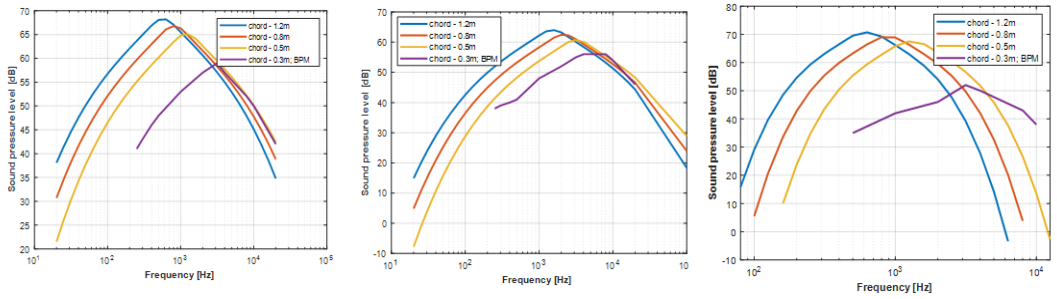

(a) (b) (c)

Figure 3. Turbulent boundary layer trailing edge, 1/3rd octave band Sound pressure level (dB), for NACA 0012 airfoil, at different chord lengths, observer distance – 1.5m and free stream velocity – 65 m/s, 4^0 AOA
(a) Suction side, (b) Pressure side, (c) Flow separation

The BPM method describes the acoustic field using the scaling laws which are correlated with boundary layer thickness, displacement and momentum thicknesses and typically expressed as function of the chord length and angle of attack. The scaling law approach helps to obtain data and perform transformation for a small model and produce valuable design information required for development of large prototype model [5].

The BPM method essentially considers five major noise mechanisms which include the turbulent boundary layer interaction with the trailing edge of airfoil, flow separation noise from suction side of airfoil, vortex shedding noise from trailing edge thickness, the tip noise and laminar boundary layer noise from pressure side of airfoil at leading edge [10], [11].

Regardless of geometry of the airfoil, any stationary or moving surface is modeled as half-infinite flat plate upon which incident pressure field undergoes edge scattering near the trailing edge. Edge scattering process results in efficient aerodynamic noise generation due to boundary layer shear present in turbulent flows. Starting from Fig. 3(a) through Fig. 3(c) it can be seen that the maximum sound pressure from the suction side of airfoil is ~68dB.

The pressure side shows a value of 64dB while the flow separation noise shows a value of 70dB. The regions of sound spectrum amplitude where the distinct peaks are observed were attributed to boundary layer instabilities or amplification of acoustic pressure fluctuations caused by diffraction at the trailing edge and its propagation downstream.

Further the amplitude of sound pressure was found to decrease with the reduction of different chord lengths, 1.2m, 0.8m and 0.5m by ~2dB. It can be noted that the amplitude is found to vary both for low and high frequency regions of the spectrum. With increasing chord length, the sound pressure level, dB was found to increase between 100-1000 Hz while, decreasing in the very high frequency regions, f>10 kHz.

The present results agreed well with the data obtained from [2], [3] for airfoils at a 5^0angle of attack in the high frequency region of spectrum for f > 5 kHz. Further, for angle dependent noise source as given by Eq. (3), the agreement of simulated data with existing data from [2] was low and was found to deviate by more than 10dB for whole spectrum.

For the pressure side of airfoil, the agreement was better and within 5dB, while for the suction side simulated data correlated well with reference data for f >5 kHz. The flow separation or stall induced noise showed a large change in the amplitude of ~ 30dB for change in the chord length of airfoil from 1.2m to 0.3m, respectively.

This difference is due to the fact that when the angle of attack is kept constant, the boundary layer flow over airfoil tends to separate over shorter distance from the leading edge

and hence the thickness of the boundary layer is lesser than when the angle of attack is increased to stall angles of attack. From the present analysis using the BPM model, it can be inferred that the change in the geometric properties of source will affect the surface acoustic pressure levels in near field as well as the sound levels perceived by observer in far field.

Further, in the next section, it will be demonstrated that model outputs are strongly dependent on the fifth power of the Mach number. The wind tunnel experiments from the BPM model [2], [3] have illustrated that free stream velocity in the tunnel, tunnel configuration i.e. the test section parameters have significant influence on the flow angle of attack. The results also varied less significantly with Reynolds number expressed as function of chord length of airfoil. For the free stream velocity of 65m/s the Reynolds number was found to vary with the chord length and it was found to be 4.83 x 10^6, 3.22 x 10^6, 2.014 x 10^6 corresponding to the chord lengths of 1.2m, 0.8m and 0.5m, respectively.

From Eq. (1) - Eq. (6) the sound levels were also modeled using Strouhal number parameter which implies that the influence of the surface acoustic pressure level varies with the dominant frequency in sound spectrum as well as with the boundary layer displacement thickness over the airfoil. For each case, the average Strouhal number was found to vary between 0.01 and 1.5. The peak Strouhal number however varied in the range of 0.5 to 12 for higher values of free stream velocity.

4.3 Mach number effect

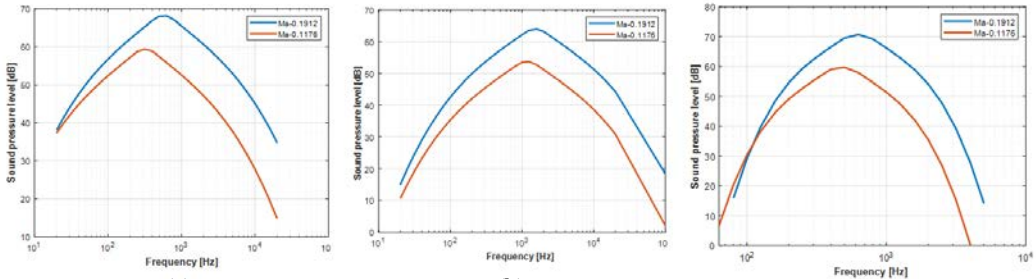

(a) (b) (c)

Figure 4. Turbulent boundary layer trailing edge, 1/3rd Octave band SPL (dB) for NACA 0012 airfoil at Mach numbers, 0.1912 and 0.1176, for chord length – 1.2m, at 4^0 AOA. Receiver position ~1.5m from trailing edge (a) Suction side, (b) Pressure side, (c) Stall separation

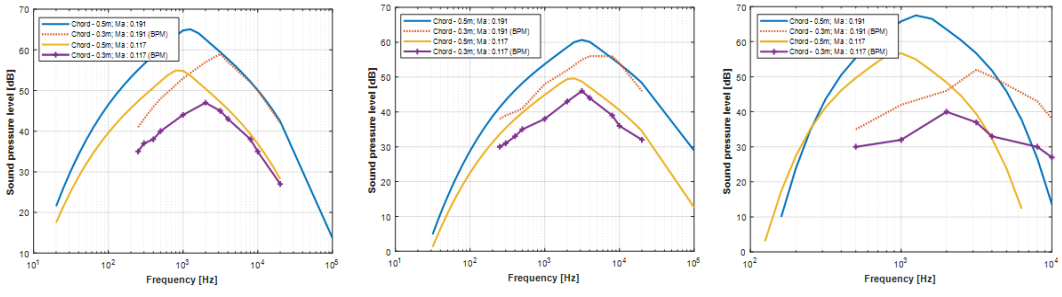

(a) (b) (c)

Figure 5. Comparison of 1/3rd Octave band TBL-TE, SPL (dB) noise for NACA 0012 airfoil of chord length 1.2m and for Mach numbers, 0.1912 and 0.1176, at 4^0 AOA with BPM data at 5^0AOA, Receiver position ~1.5m from trailing edge; (a) Suction side, (b) Pressure side, (c) Stall separation

From Fig. 4(a) through Fig. 4(c) it can be noted that the sound pressure level (SPL) increases by ~ 10dB between the 500 Hz to 1200Hz region of the spectrum for pressure,

suction sides of the airfoil due to increase in Mach number. One of the reasons which can be attributed to increase in SPL is that at low to moderate angle of attack, the boundary layer thickness increase steadily with high velocity and contributes to Sound pressure level.

Further, for low Mach number flows, the compressibility effect on the magnitude of the sound pressure level is also ignored; however it was found that the effect of compressibility varies negligibly with the angle of attack [11].

Hence, a moderate angle of attack of 4^0 was assumed for interpreting the Mach number effect on the sound pressure level.

From Fig. 5(a) through Fig. 5(c) analytical data found from ref. [2], [3] were compared with the present results which showed a better correlation for the suction and pressure sides of airfoil on the frequency region, for f >5 kHz.

For the flow separation source, a weak agreement was found between both results in terms of peak amplitude due to difference in chord length of the airfoils.

4.4 Angle of Attack effect

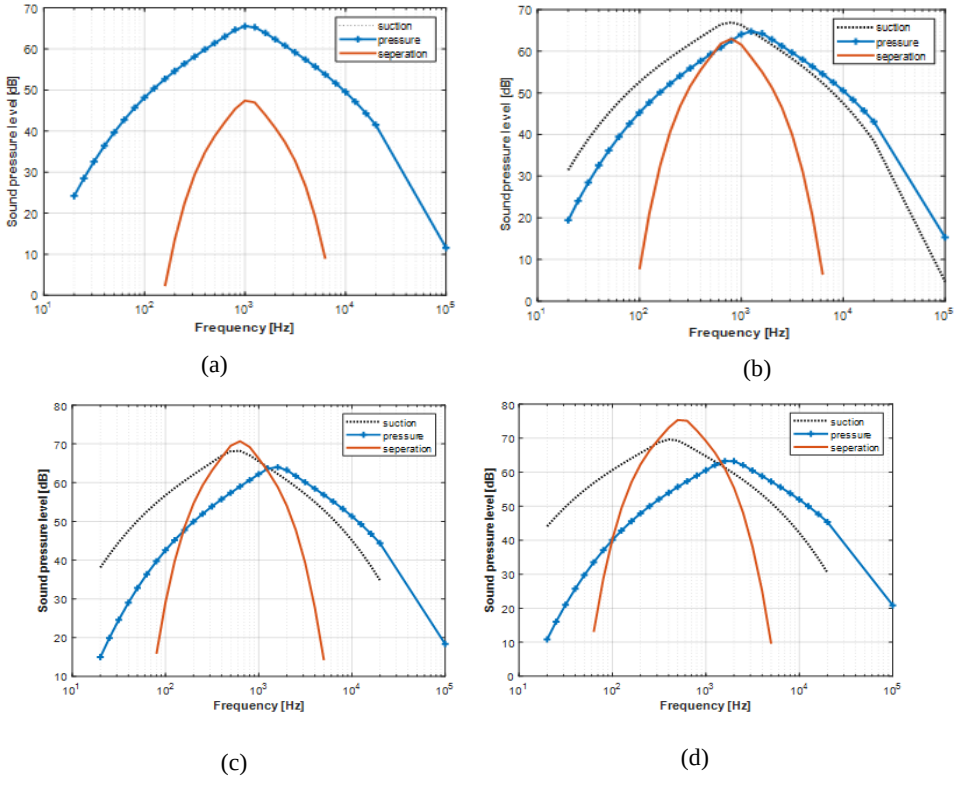

Figure 6. Turbulent boundary layer trailing edge, SPL(dB), for NACA 0012 airfoil, for chord length – 1.2m, free stream velocity, 65 m/s, Receiver position ~2m from source, for angles of attack (a) 0^0, (b) 2^0, (c) 4^0, (d) 6^0

The dependence on angle of attack on amplitude of SPL, dB for NACA 0012 is shown in Fig. 6(a) through Fig. 6(d).

It can be seen that at 0^0 AOA, the suction and pressure side SPL coincide which indicates that for symmetric airfoils the amplitude of SPL, dB remain the same over the whole spectrum. Further, from Fig. 6(d) it can be observed that the stall separation noise

becomes dominant at moderate angles of attack due to mean or strong adverse pressure gradient from the suction side of the airfoil leading to flow separation or backflow [2].

The influence of the external pressure gradients in the flow over the stationary hard surfaces are similar and comparable to flow over airfoils in open jet anechoic wind tunnels experiments or for flows encountered in canonical open channel flows such as in pipes [12], [13]. This also indicates that velocity profiles for the turbulent flows affect the boundary layer properties and also contribute to acoustic pressure via the wall pressure fluctuations [6], [12], [13].

It must be noted that for low to moderate positive angles of attack, the peak sound levels from pressure and suction side do not vary significantly when the boundary layer thickness or displacement thickness tend to increase steadily. On the contrary, for stall angles of attack, the boundary layer thickness or displacement thickness on the suction side increase higher than the pressure side. Therefore, for 200 <f < 1 kHz, an increase in sound pressure levels by 10 - 15dB for stall angles of attack due to large flow separation from suction sides of airfoil is observed. This trend can be observed for all subsonic or low Mach number flows regardless of the geometry of airfoil [2], [16].

Since the sound levels increase with the Mach number, M^5, it is evident that for a step change in the angle of attack, the dominant frequency in the spectrum remains constant without any relationship with other factors.

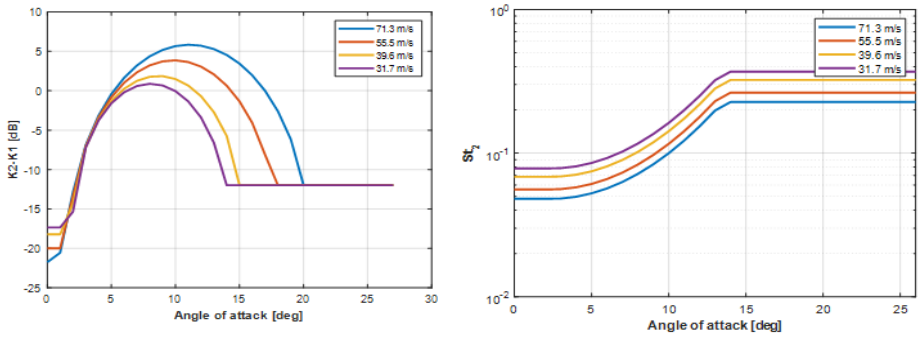

(a) (b)

Figure 7. (a) Difference in trailing edge noise amplitude functions (K2-K1) dB, between the suction and pressure sides of airfoil for Mach numbers, Ma – 0.21, 0.163, 0.116, 0.093 with varying angle of attack [0^0-26^0], (b) Peak Strouhal number variation, with angle of attack [0^0-26^0]

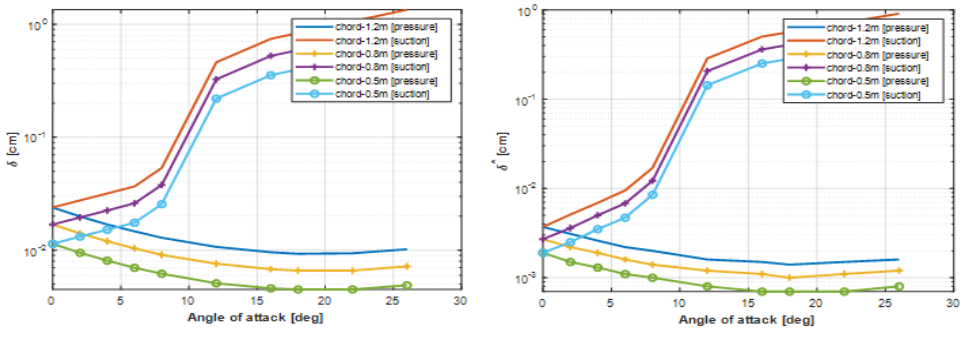

(a) (b)

Figure 8. Change in turbulent boundary layer trailing edge displacement thickness, δ* (cm) thickness, δ (cm) of NACA 0012 airfoil, for angle of attack range [0^0 - 26^0]; receiver distance ~2m from source, with chord lengths (a) Thickness-δ, at Ma = 0.1912, (b) Displacement thickness, δ*, at Ma = 0.1912

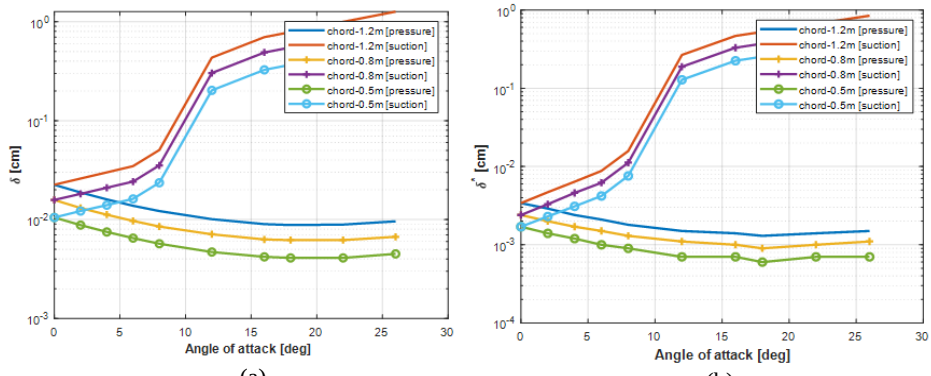

Figure 9. Change in turbulent boundary layer trailing edge displacement thickness, δ* (cm) thickness, δ (cm) of NACA 0012 airfoil, for angle of attack range [0^0 - 26^0]; receiver distance ~2m from source, with chord lengths (a) Thickness-δ, at Ma = 0.117, (b) Displacement thickness, δ*, at Ma = 0.117

Fig. 7(a) demonstrates the difference in the amplitude functions, K2-K1, between the trailing edge noise and the flow separation source for different angles of attack. At low Mach number and for subsonic flows, at low to moderate positive angles of attack, the difference was found to be negative, -5 to 10dB, while for higher positive angles of attack it varied by ~5dB. This difference was due to flow separation noise which contributes by ~ 10dB at large positive angles of attack [15]. Further, the trends for amplitude difference, K2-K1, are similar and it was found to increase with the free stream velocity. It also affects the overall amplitude of the trailing edge noise according to Eq. (1) through Eq. (3) as discussed in earlier sections. Fig. 7(b) illustrates the Strouhal number for NACA 0012 airfoil for free stream velocities, U – 71.6 m/s, 55.5 m/s, 39.6 m/s, 31.7 m/s. The Strouhal number interprets the ratio of inertial forces acting in an oscillating flow close to wall or boundary relative to the force in free stream flow. A higher value for this quantity shows that the flow is unstable or critically stable and depends on the characteristic dimension of the source. In the present study, the characteristic dimension was taken as boundary layer thickness and displacement thickness. From Fig. 8(a) and Fig. 8(b) numerical results obtained using the BPM model for NACA 0012 airfoil revealed that the thicknesses and displacement thickness on pressure side is found to decrease with AOA. On the suction side it increased steadily up to 10^0 AOA and large step increase was found after 10^0. Similar trends were observed for ratios of δ and δ* and can be found in Fig 9(a) and Fig 9(b) for M-0.117. This is attributed to the influence of the external pressure gradient, at which the onset of stall or flow separation begins to occur.

4.5 Comparison of sound power level for NACA 0012 & NACA 6320 airfoils

The thickness, δ, was observed to be ~1.2cm very near trailing edge on the suction side while for the pressure side it is 0.2mm between 12^0- 14^0 AOA. Further, it can also be noted that with increase in Reynolds number, the boundary layer thickness, δ, and δ* were found to decrease at lower AOA, however, it increases steadily with increasing AOA at given, Re. δ_0 is the boundary layer thickness at zero AOA.

The tangential velocity field for both airfoils has been computed using the boundary element method as described in ref. [14]. From Fig. 10 (a) and Fig. 10(b) the contours of sound power levels, dB, are compared for NACA 0012 airfoils for two different Mach numbers and for varying Strouhal number, St. The sound levels reached peak values between St = 0 and St = 0.5 where St = fδ/U. Similarly, from Fig. 10(c) and Fig. 10(d) the sound levels for NACA 6320 are illustrated. Further from Fig. 10(e) it can be apparent that a

difference of 2dB between symmetric and cambered profiles in the low frequency part of the spectrum, 100 Hz and 1000Hz is present however, between 1 kHz and 10 kHz, the spectral amplitude changed very negligibly (<1dB). The amplitude of the sound power level was found to increase by ~ 7dB for the entire frequency spectrum; however, any further change caused negligible amplitude fluctuation. This can be attributed to increased effective span length of the airfoil causing the turbulent boundary layer at trailing edge to radiate higher noise [16]. Also varying the effective span length changed the aspect ratio and hence the pressure amplitudes by 10dB or more. Further, in the present analysis, the boundary layer over airfoils is not tripped which affects the boundary layer transitions caused by introducing grit, tripping, suction or blowing methods aimed at noise reduction [2], [3], [16].

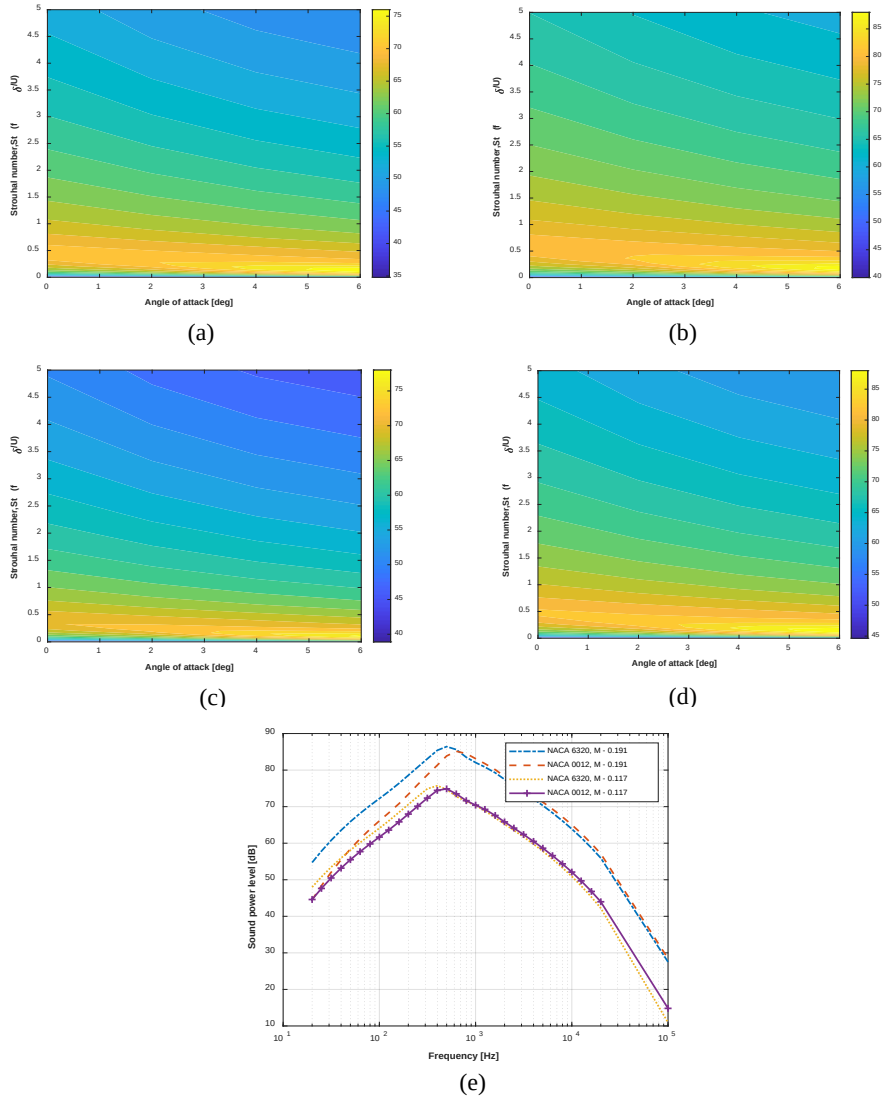

Figure 10. Contours of turbulent boundary layer trailing edge, (TBLTE) sound power level (dB) for chord length of 1.5m and aspect ratio 2 between 0^0 and 6^0 angle of attack: (a) NACA 0012 at Ma = 0.1174; (b) NACA 0012 at Ma = 0.1912; (c) NACA 6320 at Ma = 0.1174; (d) NACA 6320 at Ma = 0.1912; (e) TBLTE sound levels for the NACA 0012 and NACA 6320 aerofoils

Table 2. Maximum values for Turbulent Boundary layer - thickness, δ (mm), displacement thickness, δ*(mm) computed for NACA 0012 using BPM model, from suction and pressure side of airfoil for Mach numbers, 0.191 and 0.117 with varying chord lengths at angle of attack, $\alpha \sim 20^0$

NACA 0012		Ma – 0.191		Ma – 0.117	
		δ	δ*	δ	δ*
Chord -1.2m	Pressure	0.276	0.043	0.293	0.046
	Suction	12.67	8.47	13.43	9.09
Chord -0.8m	Pressure	0.193	0.03	0.207	0.03
	Suction	8.86	5.98	9.49	6.54
Chord-0.5m	Pressure	0.129	0.02	0.14	0.02
	Suction	5.92	4.07	6.41	4.54

5. CONCLUSIONS

Trailing edge noise from NACA 0012 and NACA 6320 showed that an increase in chord length of airfoil leads to the change in the magnitude of SPL for constant span increased by 10dB on the pressure side, ~ 8dB on the suction side and ~2dB for flow separation noise in low frequency region of spectrum. Increase in Mach number also resulted in increase of SPL by ~10dB for both pressure and suction side of airfoils. A difference of ~2 -5dB in SPL was found between the NACA 6320 and NACA 0012 airfoils for increasing Mach number near low frequency; however the peak amplitude of spectrum varied negligibly with the angle of attack. The angle dependent noise increased the pressure amplitude by nearly 2-5dB. The thickness and displacement thickness were found to increase with angle of attack for the suction and pressure sides of the airfoil but reduced with increase in chord Reynolds number and Mach number. At high frequencies, f> 5 kHz thin airfoils produced high trailing edge noise by ~2-3dB than at low frequencies and vice-versa. Thick and cambered airfoils however produced lower noise for f >5 kHz by 2dB than at low frequencies.

ACKNOWLEDGEMENT

We would also like to extend the gratitude to the institutions for providing support for the computational lab facilities in order to pursue the research.

REFERENCES

[1] R. K. Amiet, Noise due to turbulent flow past a trailing edge, *Journal of Sound and Vibration*, 1976.
[2] T. F. Brooks, T. H. Hodgson, Trailing edge noise prediction from measured surface pressures, *Journal of sound and vibration*, Volume **78**, 1981.
[3] T. F. Brookes, Pope et al, *Airfoil self-noise and prediction,* NASA Reference publication 1218, 1989.
[4] C. Doolan, et al, *Trailing edge noise production, prediction and control*, University of Adelaide, 2012.
[5] M.W. Frank, *Fluid Mechanics*, 7th edition, Mc Graw Hill Publishers Ltd, 2011.
[6] M. Goody, Empirical spectral model of surface pressure fluctuations, *AIAA Journal*, Volume **42**, No 9, 2004.
[7] N. Hu, Contributions of different aero-acoustic sources to aircraft cabin noise, *AIAA Journal*, 2013.
[8] Hu. N (2017) *Simulation of wall pressure fluctuations for high subsonic and transonic turbulent boundary layers*, DAGA, Kiel, 2017.
[9] Z. Hu, C. Morphey, N. D. Sandham, Wall pressure and shear stress spectra from direct numerical simulations of Channel flow up to Re_τ = 1440, *AIAA Journal*, University of Southampton, England, UK, DOI: 10.2514/1.17638, 2006.
[10] J. Kim, H. J. Sung, *Wall pressure fluctuations and flow induced noise in a turbulent boundary layer over bump*, Proceedings of the 3rd international conference (ICVFM 2005), Yokohama, Japan, 2005.

[11] T. Kim, et al, *Design of low noise airfoil with high aerodynamic performance for use on small wind turbines,* Science China Press and Springer-Verlag Berlin Heidelberg, 2010.
[12] B. E. McGrath, R. L. Simpson, *Some features of surface pressure fluctuations in turbulent boundary layers with zero and favorable pressure gradients,* NASA CR 4051 report, 1987.
[13] Y. Rozenberg, G. Robert, S. Moreau, Wall-Pressure Spectral Model including the Adverse Pressure Gradient Effects, *AIAA Journal*, Volume **50**, Issue 10, 2012.
[14] K. Muralidhar, A. Sundararajan, et al, *Computational methods in fluid flow and heat transfer,* Narosa publishing house, 2012.
[15] Wei et al, *Modeling of noise from wind turbines,* Department of Wind Energy, Risoe-DTU, 2005.
[16] T. Yuan, *Modeling of wind turbine noise sources and propagation in the atmosphere,* ENSTA Paris Tech University, Paris – SACLAY, Aug 2016.